Polymer 230 (2021) 124073

Contents lists available at ScienceDirect

Polymer

journal homepage: www.elsevier.com/locate/polymer

Sequential photo-thermal curing of (meth)acrylate-epoxy thiol formulations

Adrià Roig [a], Xavier Ramis [b], Silvia De la Flor [c,**], Àngels Serra [a,*]

[a] Analytical and Organic Chemistry Dpt., Universitat Rovira i Virgili, C/ Marcel·lí Domingo s/n Edif. N4, 43007, Tarragona, Spain
[b] Thermodynamics Laboratory, ETSEIB Universitat Politècnica de Catalunya, Av. Diagonal, 08028, Barcelona, Spain
[c] Dept. of Mechanical Engineering, Universitat Rovira i Virgili, Av. Països Catalans, 26, 43007, Tarragona, Spain

ARTICLE INFO

Keywords:
Dual-curing
Thiol-ene
Thiol-epoxy
Glycidylmethacrylate
UV-Curing

ABSTRACT

In this work, a novel dual-curing procedure has been developed. It is a combination of a first radical UV-initiated thiol-(meth)acrylate reaction, followed by a second thermal thiol-epoxy step catalysed by a base. Since (meth) acrylates can lead to homopolymerization by radical mechanism, the amount of thiol has to be optimized to reach cross-linked materials with T_gs above room temperature and good mechanical performance. It should be considered, that if the amount of thiol in the intermediate materials is too low, epoxy homopolymerization can take place during the second step. The use of glycidyl methacrylate in combination with trifunctional meth (acrylates) allows this system to gel in the 1st stage and avoids possible dripping or exudation of free monomers during the storage of the intermediate materials. Moreover, this compound reacts in both stages acting as a covalent coupling between (meth)acrylates and epoxy networks. We selected trimethylolpropane tris(3-mercaptopropionate) as the thiol, 2,2-dimethoxy-2-phenylacetophenone as UV initiator and 1-methylimidazole as the base catalyst.

The curing evolution was studied by DSC and FTIR. All the materials obtained were characterized by thermogravimetry, thermomechanical analysis and tensile tests.

1. Introduction

Thermosets are very important industrial materials because they cover a wide range of applications in many different fields such as coatings [1,2], adhesives [3], aerospace [4] or automobile industry [5]. Dual-curing is an efficient and versatile synthetic methodology that allows to fabricate thermoset devices or apply them in a controlled way with a broad range of characteristics. This consists in a sequential or simultaneous combination of two different curing reactions that can be initiated by different stimuli like temperature or UV-light [6]. Sequential dual-curing has many advantages but one of them is that it permits the preparation of stable intermediate materials in viscous or solid state with specific mechanical properties that can be directly applied or processed in order to get, once the second stage has been completed, a fully cured polymer with higher mechanical performance. The most traditional dual-curing system relies on a first step performed under UV-light and a second step triggered at high temperature. This is a useful procedure because it avoids the vitrification of the final material during the thermal stage since this is carried out at temperatures above the ultimate glass transition temperature (T_g) of the polymer. This type of sequential dual-curing is now implemented in the field of 3D-printing [7–12]. The most used reactions in the first stage of this type of dual-curing are thiol-ene [13,14], homopolymerization of meth (acrylates) [10,15] and cationic homopolymerization of epoxides [16,17] combined with epoxy-amine [11], epoxy-anhydride [8], homopolymerization of epoxides [18] or thiol-epoxy [19] reactions as the second stages.

Recently, a huge interest has arisen on the thiol-ene photoinitiated polymerizations. Typical monomers are allyl derivatives of bisphenol A or unsaturated fatty acids derivatives [20,21]. This reaction takes place via step-grown radical addition mechanism and implies some advantages like the promptness of the reaction, relatively high oxygen tolerance and low shrinkage, leading to highly transparent materials. Despite this, the flexible thioether bonds formed during the thiol-ene reaction as well as the flexible chain of the commercially available thiols cause some drawbacks in the final cured materials such as low T_g's, poor

* Corresponding author.
** Corresponding author.
E-mail addresses: silvia.delaflor@urv.cat (S. De la Flor), angels.serra@urv.cat (À. Serra).

https://doi.org/10.1016/j.polymer.2021.124073
Received 27 May 2021; Received in revised form 29 July 2021; Accepted 2 August 2021
Available online 3 August 2021

rigidity and hardness promoted by low modulus values [22,23]. In contrast, the photocuring of thiol-(meth)acrylate mixtures does not provide this kind of problems due to the occurrence of a competitive reaction, which is the radical (meth)acrylate homopolymerization, which follows a chain-growth mechanism [24]. Another advantage of (meth)acrylates is their good commercial availability with different structural characteristics. Whereas (meth)acrylate groups have a functionality of 1 in thiol-ene reactions, they have a functionality of 2 in the homopolymerization mechanism. This fact, increases crosslinking densities of the final networks and helps to diminish the required amount of thiol monomer in the formulation, leading to harder materials with a higher T_g. It is reported, that the kinetic constant of the radical homopolymerization of acrylates is 1.5 greater than that of the abstraction of the hydrogen of the thiol and the subsequent reaction between a thiyl radical and an acrylate [25]. This situation can generate difficulties in the calculations of the stoichiometric imbalance to reach an improvement on mechanical properties of the final thermosets.

As far as we know, very few investigations have been made in the radical thiol-(meth)acrylate/thiol-epoxy dual-curing due to the high complexity of the reaction process. Jian et al. [19] reported the synthesis of materials using a simultaneous thiol-epoxy/thiol-acrylate system. In the curing, they used 1,5,7-triazabicyclo[4.4.0]dec-5-enyl tetraphenylborate, a photobase generator which when it is irradiated by UV light is able to generate free radicals and a strong base that can trigger both reactions. Moreover, they used isopropylthiolxanthone to extend the wavelength absorption of the catalyst. However, as the photobase generator also releases the base, base-catalysed Michael addition also took place. They found that thiol-acrylate and acrylate homopolymerization were much faster than thiol-epoxy reactions and that polymerization shrinkage decreased on enhancing the thiol-epoxy mechanism, while storage modulus, glass transition temperature and hardness increased as well.

Taking all of this into account, we report a new sequential photothermal curing of (meth)acrylate-thiol-epoxy formulations based on glycidyl methacrylate (GMA) and trimethylolpropane tris(3-mercaptopropionate) (S3), using 2,2-dimethoxy-2-phenyl-acetophenone (DMPA) as UV radical initiator and 1-methylimidazole (1MI) as the catalyst for the thermal step. We also added trimethylolpropane triacrylate (TMPTA) or trimethylolpropane trimethacrylate (TMPTM) to the formulation, which have a higher functionality to obtain gelled intermediate materials during the first UV curing step. It should also be noticed, that the selection of GMA as the epoxy monomer makes this reactive system highly advantageous, due to the absence of free unreacted molecules after the first step, avoiding possible dripping or exudation during the application or storage of the intermediate materials. Moreover, GMA capable to react in both curing stages, acts as a coupling agent. The competition of the radical thiol-acrylate and acrylate homopolymerization during the first step affects the T_g of the intermediate and final materials, since it leads to the stoichiometric imbalance and to the presence of unreacted thiol groups in the final material, which reduces T_g values. On the other side, reducing the proportion of thiols in the initial formulation, the homopolymerization of unreacted epoxides, once the thiol groups are exhausted, can occur. This will increase the T_g of the final material as well as the crosslinking density. Thus, because of such a complex curing mechanism, we have optimized the formulation composition to reach the adequate characteristics of the intermediate and final materials.

The evolution of both curing stages was evaluated by calorimetry (DSC) and FTIR spectroscopy and the materials obtained have been characterized by calorimetric, thermomechanical and thermogravimetric analyses and the mechanical properties by tensile test.

2. Materials and methods

2.1. Materials

Glycidyl methacrylate (GMA) was supplied by Miwon. Trimethylolpropane trimethacrylate (TMPTM), trimethylolpropane triacrylate (TMPTA), trimethylolpropane tris(3-mercapto-propionate) (S3), 1-methylimidazole (1MI) and 2,2-dimethoxy-2-phenylacetophenone (DMPA) were provided by Sigma Aldrich and used without further purification.

2.2. Preparation of the samples

All formulations (with compositions detailed in Table 1) were prepared in 5 mL vials in approximately 2 g batches. First of all, 5 % w/w of 1MI (to GMA) and 7 % w/w of DMPA (to GMA) were weighted in a vial. Then GMA was added and the mixture was manually stirred. Once dissolved, the corresponding amount (0.2 mol/mol GMA) of TMPTM or TMPTA were added, followed by the thiol, S3. The mixtures were vigorously and manually stirred at room temperature. In this study, different proportions of S3 were added to the formulations. They were coded as G_X_Y% where G indicates the presence of GMA, X indicates TMPTA or TMPTM and Y% the amount of S3 in molar percentage in reference to the stoichiometric amount. The stoichiometry of thiol-acrylate/thiol epoxy reaction is one mol of tri (meth)acrylate per mol of thiol and 1 mol of GMA per 2/3 mol of thiol. As an example, G_TMPTA_46 % is a formulation in which GMA and TMPTA are used and a 46 % mol of S3 has been added to the mixture.

The formulations prepared, were poured in a pre-silanized glass mould and left under a 36W UV lamp during 6 min (stage 1) in time intervals of 2 min to limit the increase of temperature. At the end of this first stage, the mixtures were cured in a conventional oven at 100 °C during 2 h and post-cured at 150 °C during 1 h. Fully cured samples for dynamomechanical (DMA) and thermogravimetric (TGA) analyses were die-cut and slightly polished with sandpaper to obtain rectangular specimens of 20 × 5 × 0.8 mm^3.

2.3. Characterization techniques

Differential Scanning Calorimetry (DSC) analyses were carried out on a Mettler DSC-3+ instrument calibrated using indium (heat flow calibration) and zinc (temperature calibration) standards. Samples of approximately 8–10 mg were placed in aluminium pans with pierced lids and analyzed in nitrogen atmosphere with gas flow of 50 cm^3/min. Dynamic studies between −80 °C and 250 °C with a heating rate of 10 °C/min were performed in order to characterize the curing process. The T_gs of the intermediate and final materials were determined by

Table 1
Compositions of the formulations prepared.

Sample	GMA (mol %)	TMPTA (mol %)	TMPTM (mol %)	S3 (mol %)	1MI (mol %)	DMPA (mol %)
G_TMPTA_stoich	45.6	9.1	–	39.6	3.9	1.8
G_TMPTA_62 %	53.8	10.8		28.7	4.6	2.1
G_TMPTA_58 %	54.8	11.0	–	27.4	4.7	2.1
G_TMPTA_54 %	55.8	11.2	–	26.0	4.8	2.2
G_TMPTA_50 %	56.9	11.4	–	24.6	4.9	2.2
G_TMPTA_46 %	57.9	11.6	–	23.2	5.0	2.3
G_TMPTA_42 %	59.1	11.8	–	21.6	5.1	2.4
G_TMPTA_38 %	60.2	12.1	–	20.1	5.2	2.4
G_TMPTM_58 %	54.8	–	11.0	27.4	4.7	2.1
G_TMPTM_54 %	55.8	–	11.2	26.0	4.8	2.2
G_TMPTM_50 %	56.9	–	11.4	24.6	4.9	2.2
G_TMPTM_46 %	57.9	–	11.6	23.2	5.0	2.3
G_TMPTM_42 %	59.1	–	11.8	21.6	5.1	2.4
G_TMPTM_38 %	60.2	–	12.1	20.1	5.2	2.4

performing a scan between −80 °C or −30 °C and 250 °C with a heating rate of 20 °C/min. The reaction enthalpy (Δh) was integrated from the calorimetric heat flow signal (dh/dt) using a straight baseline with help of the STARe software.

To follow the whole curing process, a FTIR spectrometer Bruker Vertex 70 with an attenuated total reflection accessory with thermal control and a diamond crystal (Golden Gate Heated Single Reflection Diamond ATR, Specac-Teknokroma) and equipped with a mid-band liquid nitrogen-cooled mercury-cadmium-telluride (MCT) detector was used. Real-time spectra were collected in absorbance mode with a resolution of 4 cm^{-1} in the wavelength range 4000 to 600 cm^{-1} averaging 20 scans for each spectrum. The disappearance of the absorbance peak at 1636 cm^{-1} corresponding to the stretching of the C=C bond of (meth) acrylates as well as the decrease of the thiol (S–H) peak at 2570 cm^{-1} were used to confirm that the first step of the curing was complete [26]. The characteristic absorbance peak at 915 cm^{-1} corresponding to the bending of the epoxy group and the appearance of a peak at 3500 cm^{-1} related to the formation of OH groups during the thiol-epoxy reactions were used to characterize the second stage [27].

The thermomechanical properties were evaluated using a DMA Q800 (TA Instruments) with the film tension clamp. All samples were stretched under an amplitude of 10 μm and a frequency of 1 Hz using ramp temperature from −30 °C to 200 °C with a heating rate of 2 °C/min.

TGA analyses were carried out with a Mettler Toledo TGA2 thermobalance. Cured samples, weighting around 10 mg were degraded between 30 and 600 °C at a heating rate of 10 °C/min in N_2 atmosphere with a flow of 50 cm^3/min.

Final materials were tested until break in tensile mode at room temperature using an electromechanical universal testing machine (Shimadzu AGS-X) with a 1 kN load cell at 10 mm/min and using Type V samples with a thickness of 1 mm according to ASTM D638-14 standard. Three samples of each material were analyzed and the results were averaged.

3. Results and discussion

3.1. Study of the curing process

The dual-curing process that we develop in the present work consists in a first photoinitiated thiol-(meth)acrylate polymerization followed by a thermal thiol-epoxy reaction as a second stage. Acrylates can react with thiols via two different pathways depending on the catalyst and conditions used: (a) Thermal thiol-acrylate Michael addition in the presence of a base [28] or (b) radical mediated thiol-acrylate reaction that can be initiated by UV irradiation in the presence of photoinitiators such as DMPA (Scheme 1). Through both reaction pathways, the structure of the final products is identical, formed by attachment of the sulphur to the methylene carbon of the vinyl group. As it is shown in the scheme, in the UV pathway, first of all, a thiyl radical is generated by reaction of the thiol and the radical produced by the photolysis of the UV initiator (reaction a). This thiyl radical can be added to the acrylic monomer in order to form a new acrylic radical (reaction b). The radical formed either abstracts a hydrogen from the thiol forming a new thiol-acrylate product and a new thiyl radical (reaction c), or propagates through another acrylate functional group generating an acrylic radical that leads to the growing of homopolymer chains (reaction d). The occurrence of this last process leads to a stoichiometric imbalance with high proportion of thiol unreacted in the intermediate and final materials. This fact means that the T_g of the material will be reduced and the final material could evolve over time due to the presence of unreacted thiol groups.

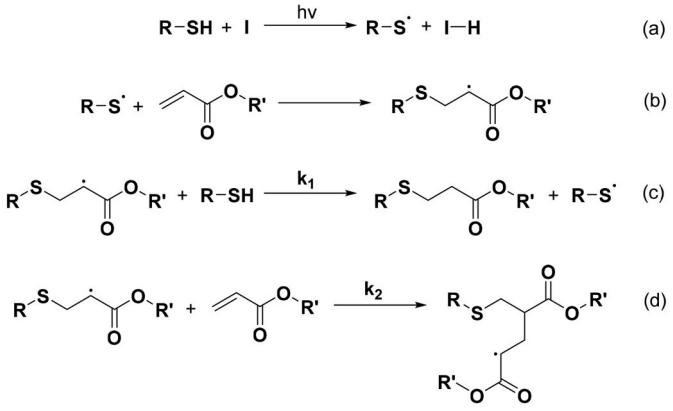

Scheme 1. Radical-mediated thiol-acrylate polymerization mechanism.

The presence of the 1-MI in the initial formulation can initiate the thio-Michael addition in concurrence with the radical UV-initiated thiol-ene mechanism. This increases the complexity of this curing process. It is worth to note, that acrylates and methacrylates have different reactivity in front of the thio-Michael addition, being acrylates more reactive since the presence of a methyl group in methacrylates makes more difficult the nucleophilic attack.

On preparing the formulation, we added to the GMA monomer, 0.2 mol of a tri(meth)acrylate, TMPTA or TMPTM, per mol of GMA to ensure gelation during the first step, and the stoichiometric amount of S3 and the initiators, DMPA and 1MI, for the first and second step, respectively. Fig. S1 shows the DSC curves of the stoichiometric formulation prepared with TMPTA after irradiation and after the second thermal step. The most representative data are collected in Table 2. We evaluated that the T_g of the intermediate material was about - 45 °C and the T_g of the completely cured material was 4 °C, being both too low for practical applications. The calorimetric curve of the intermediate material presented a well-defined exotherm with an enthalpy released of about 129 kJ per epoxy equivalent, which agrees with the previously reported for thiol-epoxy reaction [29].

To increase the T_g, the proportion of S3 in the reactive mixtures was progressively decreased and subsequently DSC studies of intermediate and final materials containing TMPTA or TMPTM were performed. Fig. 1 shows the DSC curves corresponding to the second curing step, of the photocured intermediate materials, for TMPTA formulations containing different mol % of S3 in reference to the stoichiometric amount. Fig. S2 provides the same information for parallel formulations with TMPTM. The calorimetric data are collected in Table 2.

In Fig. 1, it is possible to see an exotherm between 80 °C and 130 °C

Table 2
Main calorimetric data of the intermediate and final materials.

Sample	T_g interm (°C)	T_g final (°C)	$\Delta H_{thiol\text{-}epoxy}$ [a] (J/g)	$\Delta H_{thiol\text{-}epoxy}$ [a] (kJ/eq)	$\Delta H_{ep.\ homo.}$ [b] (J/g)	$\Delta H_{ep.\ homo.}$ [b] (kJ/eq)
G_TMPTA_stoich	−45.5	3.9	243.6	129.3	–	–
G_TMPTA_62 %	−33.7	29.8	240.5	119.1	–	–
G_TMPTA_58 %	−30.7	35.3	230.9	100.1	6.9	2.1
G_TMPTA_54 %	−26.1	39.7	217.7	89.0	15.9	7.0
G_TMPTA_50 %	−21.4	44.9	210.8	82.4	20.6	9.1
G_TMPTA_46 %	−16.9	49.0	167.6	63.3	52.4	25.6
G_TMPTA_42 %	−13.3	56.1	146.9	53.6	59.1	29.9
G_TMPTA_38 %	−11.9	59.8	137.9	48.4	73.9	31.2
G_TMPTM_62 %	−35.1		250.9	125.7	–	–
G_TMPTM_58 %	−32.1		249.1	104.4	2.1	0.9
G_TMPTM_54 %	−28.2		240.4	99.2	3.4	1.4
G_TMPTM_50 %	−26.8		225.6	90.1	11.2	4.5
G_TMPTM_46 %	−22.4		194.4	75.1	18.4	7.1
G_TMPTM_42 %	−20.8		175.2	65.3	30.2	11.3
G_TMPTM_38 %	−18.5		151.6	54.5	41.8	15.0

[a] Enthalpy released in the thiol-epoxy reaction by gram of mixture and by epoxy equivalent.

[b] Enthalpy released in the epoxy homopolymerization by gram of mixture and by epoxy equivalent.

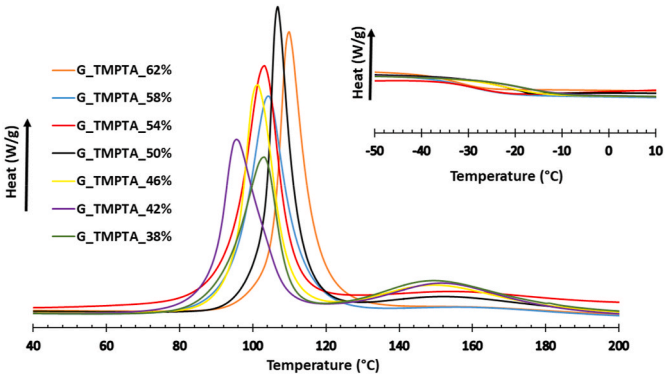

Fig. 1. DSC curves at 10 °C/min of the thermal step for the formulations containing different % mol of thiol.

corresponding to the thermal thiol-epoxy reaction. Moreover, in the formulations containing 58 % of thiol or less, a small wide peak appears between 130 °C and 175 °C. This broad exotherm can be attributed to epoxy homopolymerization, because thiols have been run out and unreacted epoxy groups are left. In the presence of 1MI, they can homopolymerize by a ring opening mechanism. We can see in Table 2 the values of enthalpies for both reactions, which are influenced by the composition of the formulation. A lower proportion of thiol in the mixture leads to a reduction of the thiol-epoxy enthalpy released and to an increase in the epoxy homopolymerization heat. Accordingly, the T_g of the TMPTA final materials increases on reducing the proportion of thiol in the formulation, due to the epoxy homopolymerization that takes place, which leads to increase the crosslinking density. It should be mentioned, that epoxide groups have a functionality of two in homopolymerization and only one in thiol-epoxy reaction, which implies an increase of the crosslinking density, when homopolymerization occurs. Moreover, the structure of S3 is quite flexible and the lower the proportion the higher the rigidity of the network. Formulations containing TMPTM released more enthalpy in the thiol-epoxy reaction, because less thiol reacts during UV-irradiation and consequently less epoxy homopolymerization occurs. The T_g of the TMPTM materials could not be determined by DSC, probably due to the higher inhomogeneity of the network obtained that did not lead to a well-defined transition. However, as it will be shown later, DMA of TMPTM formulations allows us to see this transition.

It should be deduced from Table 2, that by decreasing the amount of thiol in the formulation, the T_gs of all the intermediate materials become higher compared to those obtained from the stoichiometric formulation. Moreover, TMPTA intermediate materials have slightly higher T_gs than the TMPTM ones. This indicates that thermal thiol-Michael reaction competes with the thiol-ene during irradiation, because the heat evolved in the thiol-ene can favour this reaction, being easier for acrylate derivatives, as previously commented. Thus, less unreacted thiols are present in the formulation and consequently, T_gs are higher.

The enthalpy of the thiol-epoxy reaction is a bit higher in the case of methacrylates, because more thiol groups are left unreacted in the intermediate materials, which are able to react with epoxides. Consequently, less homopolymerization takes place, as we can see from the heat evolved in the broad exotherm at higher temperatures.

In both types of formulations, the progressive reduction of S3 proportion in the mixture produces a subsequent increase in epoxy homopolymerization, increasing the T_g of the cured materials as a result of the higher crosslinking density and the increase in the rigidity of the network. We can also see, that for higher concentrations of thiol (above 54 %) the epoxy homopolymerization is meaningless. Nevertheless, we are able to achieve materials with T_g's above room temperature either in all TMPTA formulations. However, the lower T_g of the thiol rich materials (G_TMPTA_stoich and G_TMPTA_62 %) led to these proportions being discarded for further studies.

To confirm that the reactions of each step of the dual curing have been completed, we registered the FTIR spectra of the intermediate and final materials, which were compared with the spectrum of the initial formulation. Fig. 2 shows these spectra for the G_TMPTA_58 % formulation.

As we can see, the acrylate bands at 1636 cm^{-1} and 810 cm^{-1} have disappeared in the spectrum of the intermediate materials, due to the thiol-ene, thio-Michael and (meth)acrylate homopolymerization. Therefore, the proportion of the acrylate in the formulation controls the extension of the first stage of the curing. Thiol absorption at 2576 cm^{-1} is still visible in the intermediate material, and disappears completely after the thermal process together with epoxy band at 910 cm^{-1}.

3.2. Thermal characterization of the materials

The thermal stability of the fully cured materials was evaluated by thermogravimetry. Fig. 3 shows the weight loss curves against temperature and their derivatives for TMTPA formulations. Parallel formulation with TMTPM are shown in Fig. S3 of the SI. Table 3 shows the main values extracted from the tests.

As we can see in the DTGA plot, the degradation occurs in two clearly separated steps. The presence of ester groups in the thiol and in the acrylate units could be the responsible of the first degradation step, whereas in the second the complete degradation of the network occurs. Ester groups can experiment β-elimination processes that leads to the scission of the covalent network.

The values of the initial degradation temperature in the table do not show significant differences among all the materials, but the occurrence of epoxy homopolymerization delays the initial degradation to occur and this temperature increases about 20 °C on reducing the proportion of thiol from 58 to 38% in TMPTA formulations. The effect is less noticeable in TMPTM formulations, because of the lower homopolymerization of epoxides that occurs. There is no difference in the temperature of the maximum degradation rate, but the char yields follow the tendency to increase on decreasing the thiol percentage in the formulation.

The thermomechanical characteristics of the materials were evaluated by DMTA. Fig. 4 shows the tan δ and storage moduli curves for the TMPTA materials. Fig. S4 shows parallel results for TMPTM thermosets. The main data extracted from these experiments are collected in Table 3.

The tan δ curves show a monomodal shape indicating that there is only one network structure, in spite of the various reactions taking place during the whole curing process. However, the homogeneity of the material increases as the epoxy homopolymerization decreases and the curves become narrower as it is shown in Table 3. In the same sense, the damping capacity increases, due to the higher mobility of the network

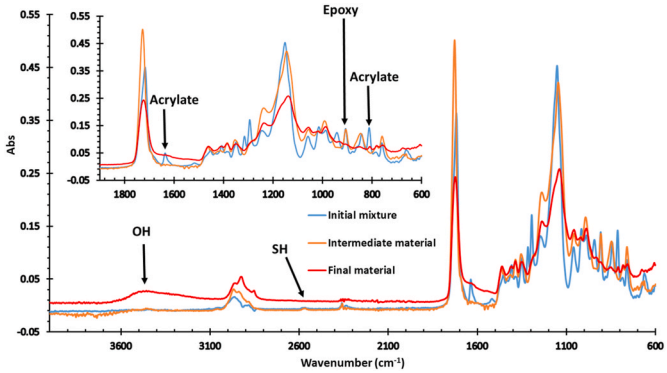

Fig. 2. FTIR spectra of initial mixture (blue), intermediate material (orange) and final material (red) of the G_TMPTA_58 % formulation. (For interpretation of the references to colour in this figure legend, the reader is referred to the Web version of this article.)

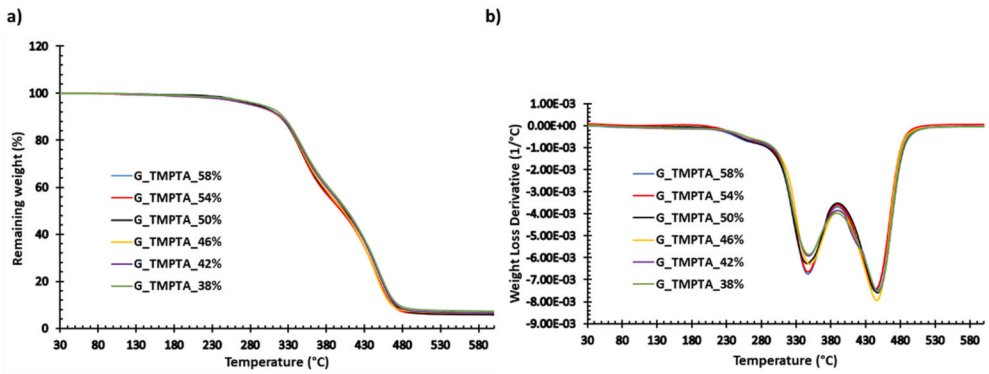

Fig. 3. TGA (a) and DTGA (b) curves for all the thermosets obtained from TMPTA formulations in N_2 atmosphere.

Table 3
Main thermogravimetric and thermomechanical data of the final materials prepared.

Sample	$T_{5\%}$[a] (°C)	T_{max}[b] (°C)	Char Yield[c] (%)	$T_{tan\ \delta}$[d] (°C)	FWHM[e] (°C)	E'_{glassy}[f] (MPa)	$E'_{rubbery}$[g] (MPa)
G_TMPTA_58 %	275	346/445	5.5	49.1	21.1	2964	28.6
G_TMPTA_54 %	277	346/446	5.6	62.1	30.6	3112	37.6
G_TMPTA_50 %	279	346/447	5.8	71.5	33.8	2957	39.1
G_TMPTA_46 %	280	347/446	6.4	75.6	36.8	2905	43.3
G_TMPTA_42 %	283	348/447	6.6	87.9	44.9	3105	53.6
G_TMPTA_38 %	295	348/448	7.3	98.8	50.9	2939	69.3
G_TMPTM_58 %	298	345/442	5.3	70.4	40.3	3100	49.2
G_TMPTM_54 %	299	345/442	5.9	76.6	42.6	2666	54.4
G_TMPTM_50 %	299	345/442	6.0	87.3	43.8	2794	55.4
G_TMPTM_46 %	300	346/442	6.4	93.8	45.6	2998	65.1
G_TMPTM_42 %	301	346/442	6.7	97.5	58.5	3500	83.1
G_TMPTM_38 %	304	346/442	6.8	112.1	61.9	2579	83.9

[a] Temperature of 5 % of weight loss.
[b] Temperature of the maximum rate of degradation of two main steps.
[c] Char residue at 600 °C.
[d] Temperature of the maximum of the tan δ peak at 1 Hz.
[e] Full width at half maximum of the tan δ peak.
[f] Glassy storage modulus determined by DMTA at −10 °C.
[g] Rubbery storage modulus determined by DMTA at 125 °C.

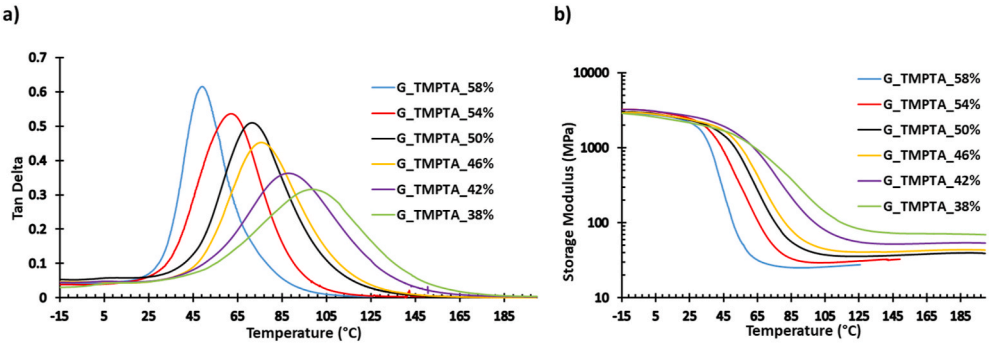

Fig. 4. Evolution of tan δ (a) and storage modulus (b) against temperature of G_TMPTA thermosets.

thanks to the higher proportion of linear aliphatic structures. A similar behaviour presents the tan δ curves in Fig. S4. In this case, the curves are broader and lower, which indicates a higher inhomogeneity of the network structure due to the higher occurrence of methacrylate homopolymerization that also leads to a lower damping capacity.

Although, the moduli in the glassy state for all the materials prepared are similar without significant differences, the values of the moduli in the rubbery state show a clear trend. The lower the proportion of thiol, the higher occurrence of epoxy homopolymerization and the higher the modulus in the rubbery state, which reflects the higher crosslinking density achieved. TMPTM materials show higher rubbery moduli than their acrylate counterparts. In these materials, less epoxy homopolymerization has been observed, but the presence of the methyl group on the methacrylate units in the network can help to increase these values.

3.3. Mechanical characterization

The mechanical characterization of all the materials prepared was performed by stress-strain experiments at room temperature in the universal testing machine. It should be mentioned that we selected only to test those materials with $T_{tan\ \delta}$ above enough with respect to room

temperature ($T_{r.t.}$) in order to obtain a comparable mechanical behaviour in glassy state. In those materials with a $T_{tan\ \delta}$ very near to $T_{r.t.}$, network relaxation can occur during the strain-stress experiment and the results will not be comparable between them.

The values of strain at break, stress at break and tensile modulus are presented graphically in Fig. 5. As it can be seen, the materials containing TMPTM show higher values of tensile modulus as well as stress at break than their TMPTA counterparts. Although in these materials there is not much epoxy homopolymerization, the presence of the methyl group in the structure of methacrylates as well as the homopolymerization of methacrylate during the UV-initiated step may produce an increase in the stiffness and the strength of the materials, which is reflected by an increase in the tensile modulus and stress at break, respectively. Moreover, it is possible to observe that the higher the proportion of S3 in the materials, the lower the values of tensile modulus and stress at break which can be attributed to the lower occurrence of epoxy homopolymerization that provides high crosslinking density and therefore more stiffness and strength to the specimens. With respect to the strain at break results, a similar behaviour is observed regardless the proportion of S3 although the rigidity is slightly higher when reducing the proportion of S3 for the same reason above mentioned. TMPTA materials present higher values in comparison to TMPTM ones because of the higher proportion of thiol-ene/thio-Michael reaction that occurs during the first step and therefore more flexible chains are present in these materials that provides to the materials more flexibility.

4. Conclusions

A novel dual curing procedure, consisting in a first UV initiated step followed by a thermal process, has been implemented. Thermosets based on meth (acrylate)-epoxy thiol formulations containing 2,2-dimethoxy-2-phenylacetophenone (DMPA) and 1-methylimidazole (1MI) as UV and thermal initiators, have been cured and characterized. Tri (meth)acrylates (TMPTA and TMPTM) used as the limiting monomers that allow the control of the extension of the first curing stage and the characteristics of the intermediate material.

The use of glycidyl methacrylate (GMA) in combination with trifunctional meth (acrylates) allows this system to gel in the first stage and avoids possible dripping or exudation of free monomers during the storage of the intermediate materials.

In the UV stage a thiol-ene reaction occurs (meth)acrylate groups and thiols, although (meth)acrylate homopolymerization competes. In case of formulations of TMPTA, thermal thio-Michael reaction was detected, because of the presence of 1MI in the initial mixture that catalyzes this reaction.

The concurrence of the (meth)acrylate homopolymerization leads to a stoichiometric imbalance in the second stage, in which thiol-epoxy reaction occurs and consequently lead to materials with T_g below or around room temperature. To increase this parameter, lower proportions of thiol were added to the formulation, but the scarcity of thiol leads to the occurrence of epoxy homopolymerization catalysed by the base. This homopolymerization increases the crosslinking density, tan δ temperature and modulus in the rubbery state.

TMPTM formulations experiment less epoxy homopolymerization than their corresponding TMPTA formulations since methacrylates homopolymerize in a lesser extent than acrylates and consequently a higher proportion of unreacted thiol is present in the intermediate material, able to react with epoxides.

The higher the proportion of thiol in the formulation the lower the tan δ temperature of the thermoset and the higher the damping characteristics and the homogeneity of the material. TMPTM thermosets show higher rubbery moduli and tan δ temperatures than their acrylate counterparts.

The characterization of the tensile properties at room temperature reveals an increase in stiffness and strength when reducing the proportion of trithiol due to the epoxy homopolymerization in both TMPTM and TMPTA, although higher values are obtained in TMPTM samples due to the presence of the methyl group in the structure and the higher proportion of homopolymerization of methacrylate during the first UV step. The occurrence of thiol-ene/thio-Michael reaction in TMPTA samples produces higher strain at break than TMPTM material, more evident for higher proportion of trithiol.

To sum up, a wide range of properties can be obtained combining glycidyl methacrylate with trifunctional (meth)acrylates and thiol compounds. The use of off-stoichiometric (meth)acrylates-epoxy thiol formulations is a useful strategy that allows tailoring the properties of the intermediate and final materials when (meth)acrylate homopolymerization competes with radical UV-initiated thiol-(meth)acrylate

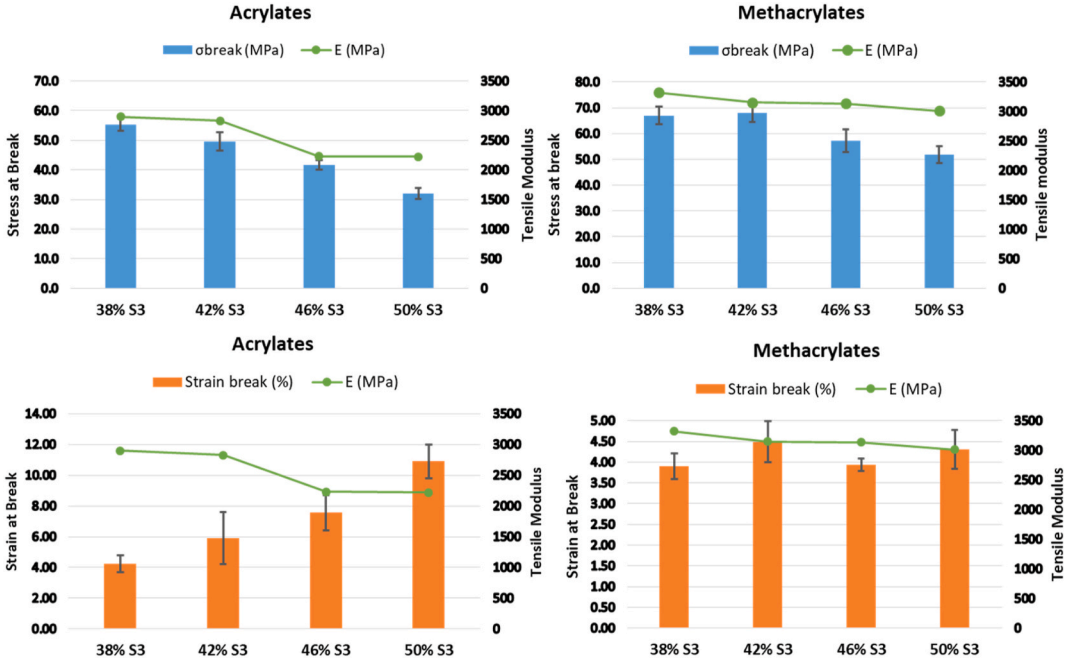

Fig. 5. Strain and stress at break and tensile modulus for the thermosets obtained from TMPTA and TMPTM materials.

reaction.

Declaration of competing interest

The authors declare that they have no known competing financial interests or personal relationships that could have appeared to influence the work reported in this paper.

Acknowledgments

The authors would like to thank MINECO (Ministerio de Economia, Industria y Competitividad, MAT2017-82849-C2-1-R and 2-R) and Generalitat de Catalunya (2017-SGR-77 and BASE3D) for their financial support. Miwon Spain S.L. is thanked for donating glycidyl methacrylate.

Appendix A. Supplementary data

Supplementary data to this article can be found online at https://doi.org/10.1016/j.polymer.2021.124073.

Author credit statement

Adrià Roig conducted the experiments and wrote the original draft. Xavier Ramis validated the studies and developed some methodologies. Silvia De la Flor and Angels Serra made the conceptualization and supervised the work. Silvia De la Flor, Xavier Ramis and Angels Serra reviewed and edited the final manuscript.

References

[1] M. Decostanzi, J. Lomège, Y. Ecochard, A.S. Mora, C. Negrell, S. Caillol, Fatty acid-base cross-linkable polymethacrylate coatings, Prog. Org. Coating 124 (2018) 147–157, https://doi.org/10.1016/j.porgcoat.2018.08.001.

[2] D. Guzmán, X. Ramis, X. Fernández-Francos, S. De la Flor, À. Serra, Preparation of new biobased coatings from triglycidyl eugenol derivative through thiol-epoxy click reaction, Prog. Org. Coating 114 (2018) 259–267, https://doi.org/10.1016/j.porgcoat.2017.10.025.

[3] S. Panchireddy, J.-M. Thomassin, B. Grignard, C. Damblon, A. Tatton, C. Jerome, C. Detrembleur, Reinforced poly(hydroxyurethane) thermosets as high performance adhesives for aluminium substrates, Polym. Chem. 8 (2017) 5897–5909, https://doi.org/10.1039/C7PY01209H.

[4] I. Hamerton, J. Kratz, The use of thermosets in modern aerospace applications, in: Qipeng Guo (Ed.), Thermosets Structure, Properties and Applications, second ed., Elsevier, Amsterdam, Netherlands, 2018 (Chapter 9).

[5] J. Verrey, M.D. Wakeman, V. Michaud, J.A.E. Månson, Manufacturing cost comparison of thermoplastic and thermoset RTM for an automotive floor pan, Composites Part A 37 (2006) 9–22, https://doi.org/10.1016/j.compositesa.2005.05.048.

[6] X. Ramis, X. Fernández-Francos, S. De la Flor, F. Ferrando, À. Serra, Click-based dual-curing thermosets and their application, in: Q. Guo (Ed.), Thermosets Structure, Properties and Applications, second ed., Elsevier, Amsterdam, Netherlands, 2018 (Chapter 16).

[7] B.J. Poelma, J. Rolland, Rethinking digital manufacturing with polymers, Science 9 (2017) 1820–1829, https://doi.org/10.1126/science.aaq1351.

[8] X. Kuang, Z. Zhao, K. Chen, D. Fand, G. Kang, H.J. Qi, J. Qi Hang, High-speed 3D printing of high-performance thermosetting polymers via two-stage curing, Macromol. Rapid Commun. 39 (2018) 1700809, https://doi.org/10.1002/marc.201700809.

[9] G. Griffini, M. Invernizzi, M. Levi, G. Natale, G. Postiglione, S. Turri, 3D-printable CFR polymer composites with dual-cure sequential IPNs, Polymer 91 (2016) 174–179, https://doi.org/10.1016/j.polymer.2016.03.048.

[10] K. Chen, X. Kuang, V. Li, G. Kang, H.J. Qi, Fabrication of tough epoxy with shape memory effects by UV-assisted direct-ink write printing, Soft Matter 14 (2018) 1879–1886, https://doi.org/10.1039/C7SM02362F.

[11] O. Konuray, F. Di Donato, M. Sangermano, J. Bonada, A. Tercjak, X. Fernández-Francos, À. Serra, X. Ramis, Dual-curable stereolithography resins for superior thermomechanical properties, Express Polym. Lett. 14 (2020) 881–894, https://doi.org/10.3144/expresspolymlett.2020.72.

[12] X. Fernández-Francos, O. Konuray, X. Ramis, À. Serra, S. De la Flor, Enhancement of 3D-printable materials by dual-curing procedures, Materials 14 (2021) 107–129, https://doi.org/10.3390/ma14010107.

[13] L. Chen, W. Quingyang, W. Guo, L. Ren, L. Zhiquan, Highly stable thiol-ene systems: from their structure-property relationship to DLP 3D printing, J. Mater. Chem. C 6 (2018) 11561–11568, https://doi.org/10.1039/C8TC03389G.

[14] C.C. Cook, E.J. Fong, J.J. Schwartz, D.H. Porcincula, A.C. Kaczmarek, J.S. Oakdale, B.D. Moran, K.M. Champley, C.M. Rackson, A. Muralidharan, R.R. McLeod, M. Shusteff, Highly tunable thiol-ene photoresins for volumetric additive manufacturing, Adv. Mater. 32 (2020) 2003376, https://doi.org/10.1002/adma.202003376.

[15] J.J. Weigand, C.I. Miller, A.P. Janisse, O.D. Mcnair, K. Kim, J.S. Wiggins, 3D printing of dual-cure benzoxazine networks, Polymer 189 (2020) 122193, https://doi.org/10.1016/j.polymer.2020.122193.

[16] C. Noè, S. Malburet, E. Milani, A. Bouvet-Marchand, A. Graillot, M. Sangermano, Cationic UV-curing of epoxidized cardanol derivatives, Polym. Int. 69 (2020) 668–674, https://doi.org/10.1002/pi.6031.

[17] M.S. Malik, S. Schlögl, M. Wolfahrt, M. Sangermano, Review on UV-induced cationic frontal polymerization of epoxy monomers, Polymers 12 (2020) 2146, https://doi.org/10.3390/polym12092146.

[18] R. Yu, X. Yang, Y. Zhang, X. Zhao, X. Wu, T. Zhao, Y. Zhao, W. Huang, Three dimensional printing of shape memory composites with epoxy-acrylate hybrid photopolymer, ACS Appl. Mater. Interfaces 9 (2017) 1820–1829, https://doi.org/10.1021/acsami.6b13531.

[19] Y. Jian, Y. He, Y. Sun, H. Yang, W. Yang, J. Nie, Thiol-epoxy/thiol-acrylate hybrid materials synthesized by photopolymerization, J. Mater. Chem. C. 1 (2013) 4481–4489, https://doi.org/10.1039/C3TC30360H.

[20] Y.H. Zhao, S. Hupin, L. Lecamp, D. Vuluga, C. Alfonso, F. Burel, C. Loutelier-Bourhis, Thiol-ene chemistry of vegetable oils and their derivatives under UV and air: a model study by using infrared spectroscopy and mass spectrometry, RSC Adv. 7 (2017) 3343, https://doi.org/10.1039/C6RA25633C.

[21] J. Zhang, L. Chunhai, J. Cheng, M. Miao, D. Zhang, Simultaneous toughering and strengthening of diglycidyl ether of bisphenol A using epoxy-ended hyperbranched polymers obtained from thiol-ene click reaction, Polym. Eng. Sci. 58 (2017) 1703–1709, https://doi.org/10.1002/pen.24767.

[22] M. Sangermano, M. Cerrone, G. Colucci, I. Roppolo, R. Acosta Ortiz, Preparation and characterization of hybrid thiol-ene/epoxy UV-thermal dual-cured systems, Polym. Int. 59 (2010) 1046–1051, https://doi.org/10.1002/pi2822.

[23] H. Matsushima, J. Shin, C.N. Bowman, C.E. Hoyle, Thiol-isocyanate-acrylate ternary networks by selective thiol-click chemistry, J. Polym. Sci., Part A: Polym. Chem. 48 (2010) 3255–3264, https://doi.org/10.1002/pola.24102.

[24] C.R. Morgan, F. Magnotta, A.D. Ketley, Thiol/ene photocurable polymers, J. Polym. Sci. Polym. Chem. Ed. 15 (1977) 627–645, https://doi.org/10.1002/pol.1977.170150311.

[25] N.B. Cramer, C.N. Bowman, Kinetics of thiol-ene and thiol-acrylate photopolymerizations with real-time Fourier transform infrared, J. Polym. Sci. Part A Polym. Chem. 39 (2001) 3311–3319, https://doi.org/10.1002/pola.1314.

[26] C. Russo, À. Serra, X. Fernández-Francos, S. De la Flor, Characterization of sequential dural-curing of thiol-acrylate-epoxy systems with controlled thermal properties, Eur. Polym. J. 112 (2019) 376–388, https://doi.org/10.1016/j.eurpolymj.2018.12.048.

[27] R. Thomas, C. Sinturel, J. Pionteck, H. Puliyalil, S. Thomas, In-situ cure and cure kinetic analysis of a liquid rubber modified epoxy resin, Ind. Eng. Chem. Res. 51 (2012) 12178–12191, https://doi.org/10.1021/ie2029927.

[28] W. Xi, C. Wang, C.J. Kloxin, C.N. Bowman, Nitrogen-centered nucleophile catalysed thiol-vinylsulfone addition, another thiol-ene “click” reaction, ACS Macro Lett. 1 (2012) 811–814, https://doi.org/10.1021/mz3001918.

[29] D. Guzmán, X. Ramis, X. Fernández-Francos, A. Serra, New catalysts for diglycidyl ether of bisphenol A curing based on thiol–epoxy click reaction, Eur. Polym. J. 59 (2014) 377–386, https://doi.org/10.1016/j.eurpolymj.2014.08.001.